

~~ATS-773~~

Table of Contents

	Page
Abstract.....	1
Introduction.....	2
Background.....	2
Previous Fracture Mapping.....	6
Methods.....	9
Results and Discussion.....	12
Main Access Drift.....	15
Tail Drift.....	19
Recommendations.....	19
Acknowledgments.....	21
References.....	22
Appendix A.....	23
Appendix B.....	28

DISCLAIMER

This document is prepared for the use of the Department of Energy. The United States Government is authorized to reproduce and distribute reprints for government purposes not withstanding any copyright notation that may appear hereon. This document is prepared for the use of the Department of Energy. The United States Government is authorized to reproduce and distribute reprints for government purposes not withstanding any copyright notation that may appear hereon.

HYDROLOGY DOCUMENT NUMBER 133

ABSTRACT

As part of LLNL's program on radionuclide migration through fractured rock, major geologic discontinuities have been mapped and characterized at the 420 m level in the Climax Stock, adjacent to LLNL's Spent Fuel Test. Persistence or continuity of features was the principal sampling criterion, and ninety major fractures and faults were mapped in the main access and tail drifts. Although the purpose and nature of this study was different from previous fracture surveys in the Climax Stock, the results are generally consistent in that three predominant fracture sets are identified: NW strike/vertical, NE strike/vertical, NW strike/subhorizontal. The frequency of major features in the main access drift is somewhat higher than in the tail drift. Those mapped in the main access drift are generally braided, stepped, or en echelon, while those in the tail drift appear to be more distinct and planar. Several of the fractures in the tail drift lie in the NE/vertical set, while most form an entirely different set oriented N5E/55NW. Sub-horizontal fractures were common to both drifts. An area of seepage associated with some of these low-angle features was mapped in the main access drift.

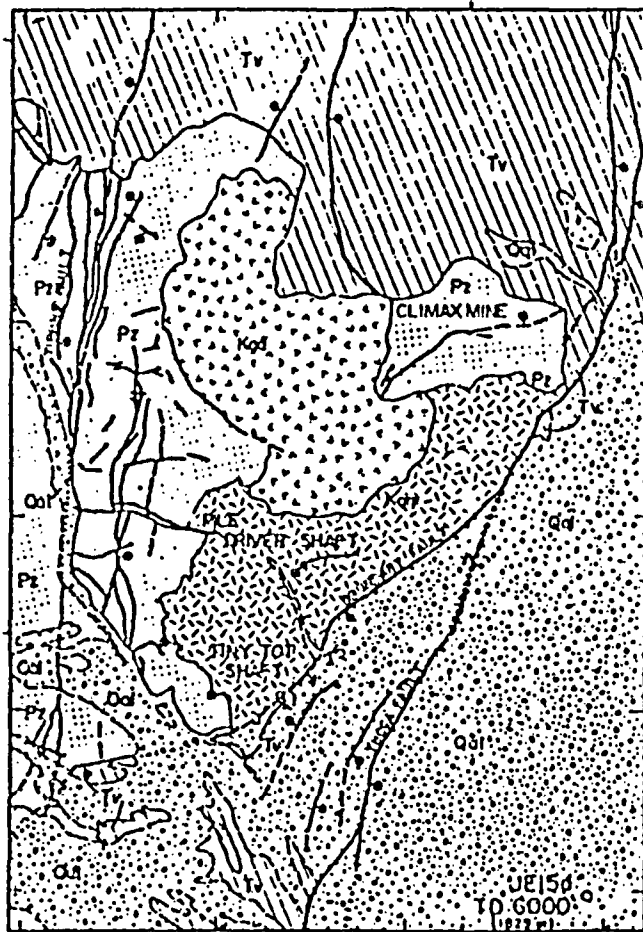
INTRODUCTION

The migration of radionuclides through geologic media is a key issue in the underground disposal of nuclear wastes. LLNL is conducting a combined field and laboratory research project to understand the transport characteristics of fractured granitic rock (Isherwood, et al. 1980). Part of this work involves circulating radionuclide-spiked groundwater through single natural fractures at depth, which understandably requires some knowledge of their geologic and geometric properties. Ideally, isolated fractures that can be intercepted and tested several meters from an entry are sought. A geologic data base for helping in the selection of experimental sites is provided by this report.

The field project is located in the Climax Stock at the Nevada Test Site (Fig. 1), near LLNL's Spent Fuel Test (Ramspott, et al. 1979). Preliminary hydrologic testing is in progress for several fractures intersecting the main access drift, and additional sites are being considered in the areas shown in Fig. 2. Maps of the major discontinuities in these drifts are included in the report and pertinent geologic information is provided. Some comparison with previous mapping projects in the Climax Stock is made.

BACKGROUND

Figure 1 is a generalized geologic map of the Climax Stock and its surroundings. The geologic setting is a composite stock of Cretaceous age that intrudes paleozoic sediments and metasediments. The majority of the exposed wall rocks are Ordovician limestones and dolomites of the Pogonip Group. The stock also intrudes the Eleana Formation, a series of argillites,



EXPLANATION



ALLUVIUM (QUATERNARY)



VOLCANIC TUFF, UNDIFFERENTIATED (TERTIARY)



QUARTZ MONZONITE, CLIMAX STOCK (CRETACEOUS)



GRANODIORITE, CLIMAX STOCK (CRETACEOUS)



LIMESTONE, DOLOMITE, SHALE, AND QUARTZITE, UNDIVIDED (PALEOZOIC)



CONTACT--Dashed where approximately located



FAULT--Dashed where approximately located. Dotted where concealed. Bar and ball on downthrown side



SHAFT

UE15d ○
TD 6,000
(1,829 m)

DRILL HOLE--Showing total depth in feet, meters in parenthesis

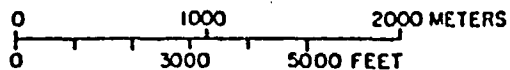


Figure 1. Geologic map of the Climax Stock.
(Modified after Barnes et.al., 1963).

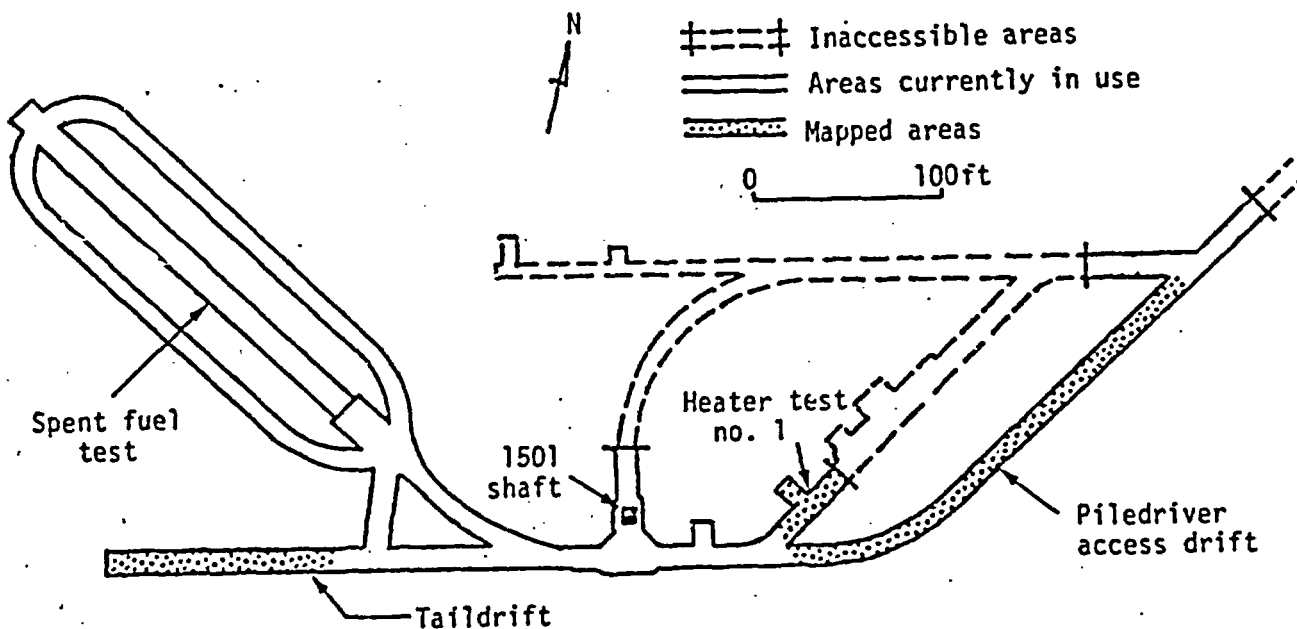


Fig. 2. Layout of drifts at 420 meter level of Climax Stock, NTS, showing areas included in the reconnaissance mapping.

limestones, and quartzites of Carboniferous age and the Cambrian Stirling Quartzite (Houser and Poole, 1960). The stock and the rocks it intrudes are overlain by the Tertiary pyroclastic rocks of the Oak Spring Formation. The stock itself is intruded by numerous aplite and pegmatite dikes.

The Nevada Test Site is in a tectonically active region of normal faulting. Three major normal faults are located near or adjacent to the stock. The Boundary Fault borders the stock on the southeast, with its east side downdropped relative to the west side. The northerly-trending Yucca Fault is also downdropped on the east side, and may connect with the Boundary Fault as shown in Fig. 1. The Tippinip Fault strikes north-northeast and is located approximately 1 km west of the stock. Its west block is downdropped relative to the east block. The Boundary and the Tippinip faults intersect southwest of the stock.

The stock consists of two major units; a quartz monzonite and a granodiorite. From cross-cutting structural relationships, Houser and Poole (1961) concluded that the quartz monzonite is the younger unit. Though the textures vary, each of the units is dominated by one textural type. The quartz monzonite is light to medium gray and porphyritic. The largest phenocrysts are euhedral orthoclase and vary in size from 2 to 10 cm. They commonly contain poikilitic inclusions of quartz, plagioclase, and biotite (unpublished thin-section data, J. Springer, 1980). Dipyramidal euhedral and subhedral quartz crystals vary in size from 0.2 to 1.5 cm. The matrix is plagioclase, quartz, K-feldspar, and biotite. Plagioclase is euhedral to anhedral, zoned, and displays polysynthetic twinning. It varies in size from 1/4 to 5 mm. Interstitial quartz is anhedral and less than 1/4 mm across.

One-quarter to 2 mm K-feldspar is subhedral to euhedral. Biotite occurs as 1/4 to 2 mm flakes within the matrix. Hornblende, sphene, and apatite are euhedral, less than 1/4 mm, and occur in trace amounts.

The granodiorite is also porphyritic and quite similar to the quartz monzonite except for the conspicuous absence of the large orthoclase phenocrysts. Hornblende is more common, though it still represents less than 1% of the rock.

Previous Fracture Mapping

Several different fracture surveys have been conducted in the Climax Stock. Maldonado (1977) states that three prominent joint sets were mapped by Houser and Poole (written communication to Maldonado, 1962) with mean orientations N32W/22NE, N64W/vertical, and N35E/vertical. He also reports similar sets found by Ege & Davis (written communication to Maldonado, 1964) at the surface of the Tiny Tot site (Fig. 1). Their orientations are N62W/20NE, N30E/vertical, and N69W/85NE. Figure 3 shows the mean pole orientations for these six joint sets plotted on an equal-area stereographic projection.

For the quartz-monzonite portion of the Pile Driver tunnel complex, Maldonado gives the average orientations of 239 faults, based on unpublished data by W. L. Emerick (1966). These data are also plotted in Fig. 3, and the ranges in strike and dip (from Maldonado's Table 10) around the dominant pole directions are indicated. The diagram shows that most of the mean fault orientations in the quartz-monzonite, which includes the area of the present study, are within 25° of the three joint sets cited above. Considering the usual scatter of poles about a mean, the correlation is fairly strong.

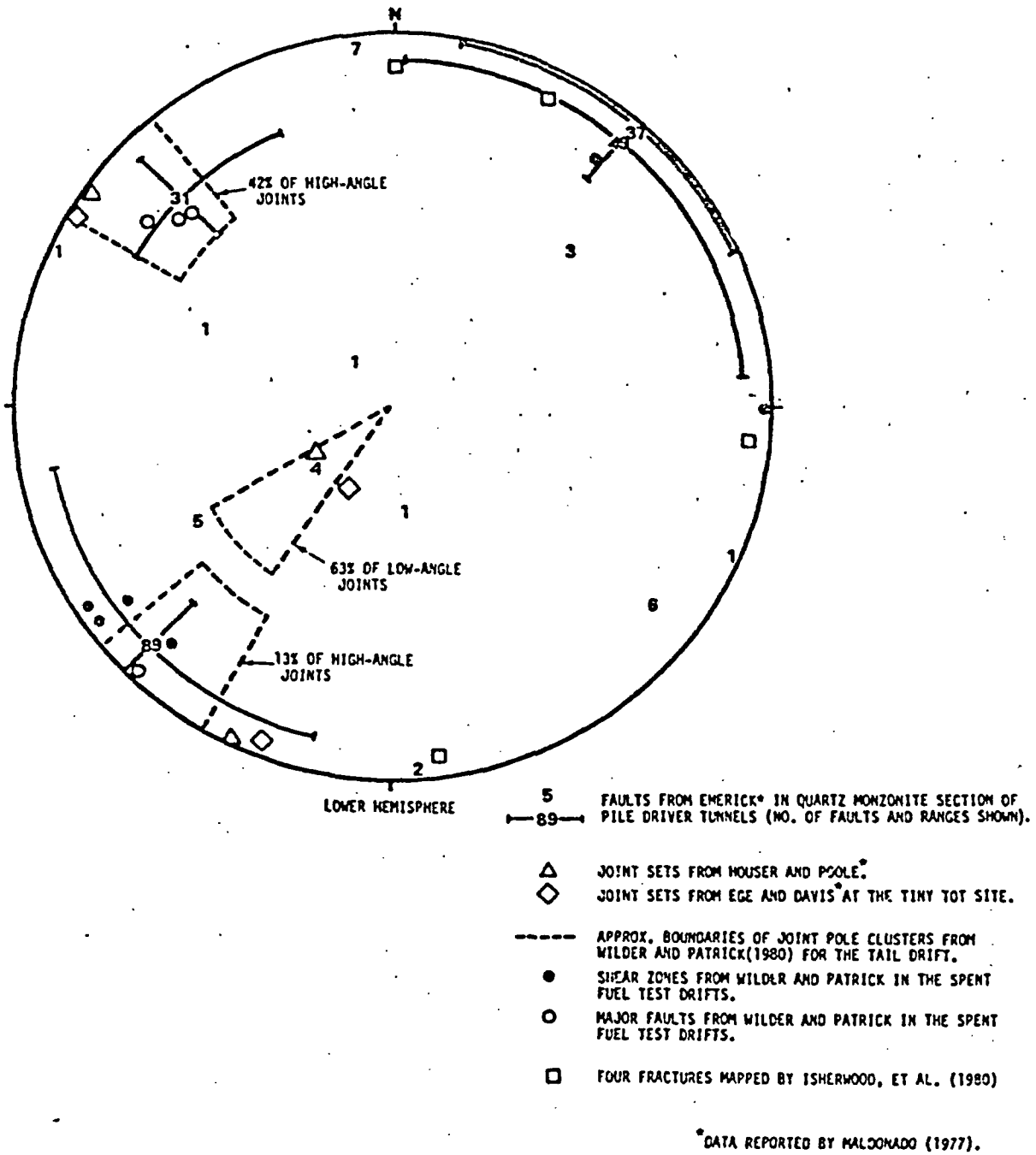


Fig. 3. Equal-area pole plot summarizing fracture orientations found in previous surveys of the Climax Stock.

Maldonado also reported three definite joint sets found by Emerick in the Pile Driver tunnels. The most prominent of these strikes from N30W to N75W. Based on the fracture map presented by Maldonado, this set is assumed to be high-angle. Another joint set strikes northeast and dips 45-80 SE. The least prominent set is subhorizontal (low-angle) with dips in the northeast quadrant. Again, these three joint sets are generally consistent with the major sets in Fig. 3.

Detailed fracture mapping has recently been done in the tail drift and the drifts being used for the Spent Fuel Test (Fig. 2). Preliminary results have been published by Wilder and Patrick (1980) and Carlson, et al. (1980), and a more complete report is in preparation. Based on strike frequency diagrams given by Wilder and Patrick for joints mapped in the tail drift, boundaries of the principal pole directions are shown by the dashed lines in Fig. 3. The low-angle joints correlate well with low-angle sets given by Maldonado. Nearly half of the high-angle joints strike roughly northeast and dip between 65SE and vertical. About thirteen percent of the high-angle fractures strike northwest and dip to the northeast. As shown by Fig. 3, these two joint sets correspond in orientation to the main sets in the Climax Stock. However, the predominance of northeast-striking joints in the tail drift is opposite from Maldonado's data, in which the northwest-striking fractures are the most numerous. Wilder and Patrick (1980) indicate that this difference in frequency is probably due to sampling bias caused by the direction of the tail drift.

The spent fuel test mapping also identified a number of high-angle shear zones and faults throughout the experiment drifts. Based on a map of these features in Wilder and Patrick (1980, Fig. 8), we have plotted the orientations as the open and solid dots in Fig. 3. The general correlation with Maldonado's fault sets is readily apparent.

In the preliminary stages of the radionuclide migration project, four prominent, high-angle fractures were mapped and characterized on the southeast rib of the main access drift (Isherwood, et al., 1980). Three sets of boreholes were drilled to intersect these fractures, and initial flow tests have been performed on two of the 3 sets of boreholes in preparation for later radio-nuclide migration experiments. Our mapping includes these four fractures, and their pole orientations are plotted in Fig. 3. Only one of these falls into the major joint sets for the stock.

METHODS

The study is concerned with major fractures that could be capable of conducting appreciable amounts of water. Small discontinuous fractures with little interconnection and fractures that appear to be induced by mining activities are omitted; only large-scale, continuous features have been studied. As criteria for sampling, features with one or more of the following properties were chosen: (1) fractures that can be traced from the base of one rib, across the ceiling, and down to the base of the opposite rib; (2) zones of parallel, braided, stepped, and/or en echelon fractures that can be traced from the base of one rib, across the ceiling and down to the base of the opposite rib; (3) features that are nearly parallel to the drift and can be traced for a distance of about twice the width of the drift; and (4) features that appear strong enough to meet one of the first three criteria, but are truncated by another major feature.

In this report the term "fracture" refers to the broad class of discontinuities resulting from mechanical failure of the rock, including cracks, joints, and faults. Fractures that exhibited clear signs of shear movement, such as slickensiding or offset of other features, are called

faults. Because shearing was difficult to discern in most instances, the other major features were simply called "fractures" rather than the more exclusive term "joints."

Orientations of fractures were measured according to the procedure given by Compton (1962). First, a level line of sight along the fracture surface is measured from about 10 feet from the fracture outcrop on the rib, and this is taken as the strike. The dip is measured along the same level line of sight from the same location by holding the compass at arm's length, then lining its edge up with the fracture trace. For low-angle fractures, a clear ink mark was made on the rock next to the fracture where the level line of sight was made. Compton suggests that this method is more accurate than the conventional method of placing the compass on the fracture surface because the irregularities on the surface are not measured, plus it is usually easier to avoid metal objects that deflect the compass needle.

Figure 4 schematically shows how the fractures were projected onto the floor map. Continuous features were mapped in plan view according to their intersection with the floor of the drift. Since the floors of the drifts are not exposed, the intersections were inferred by extrapolating between traces in the ribs. For fractures that are continuous and well-defined, the technique is quite reliable; however, it is less reliable for major features that are truncated, parallel to the drift or otherwise not visible in opposite ribs. In these cases the traces in the floor must be extrapolated from outcrops in only one rib or in the roof of the drift. Uncertainty arising from such measurements or extrapolations were noted in the mapping.

Along the access drift from station 1+10 to station 1+85 water can be seen seeping from low-angle discontinuities. In order to show the relation of the wet and dry features in this area, an additional map of part of the southwest rib was prepared. This appears as section A-A' on the fracture map which is discussed in the following section.

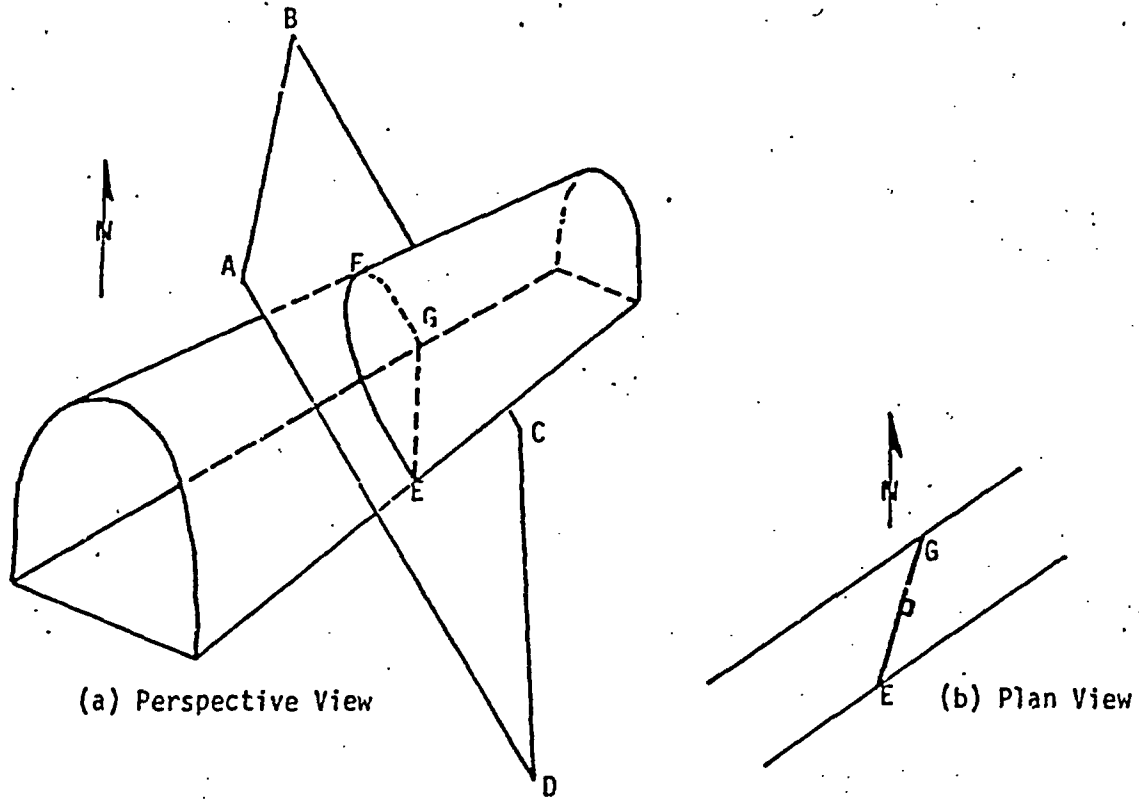


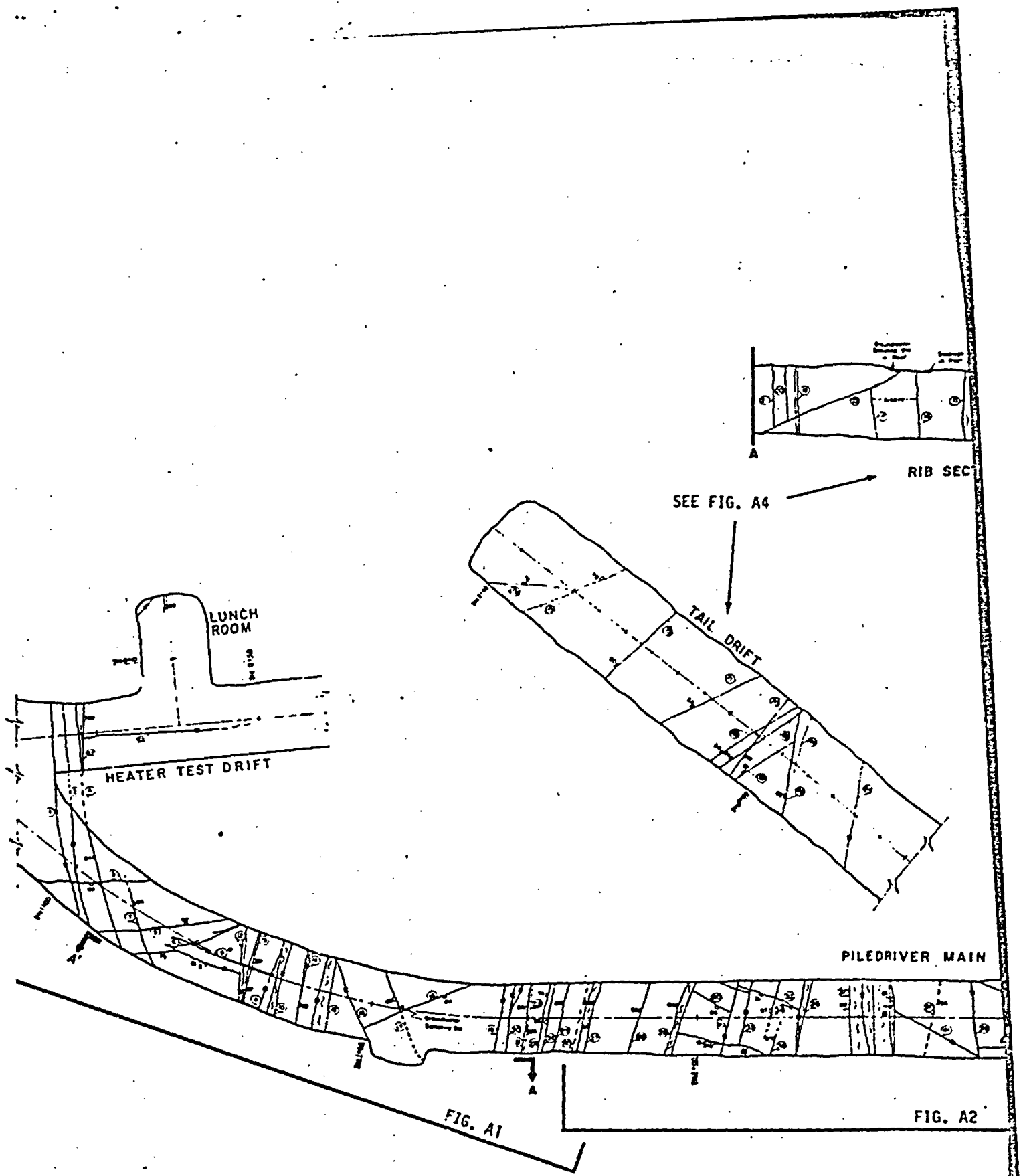
Fig. 4. Schematic diagram of mapping technique. Fracture plane ABCD in (a) strikes NNE and dips steeply to the east. Its intersection with the drift is the trace line EFG, and the mapped representation of the fracture in plan view is shown in (b).

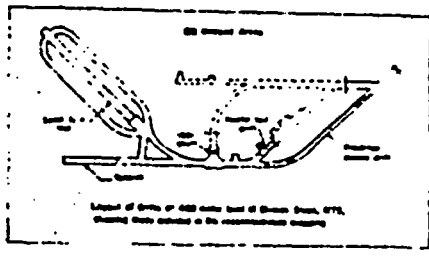
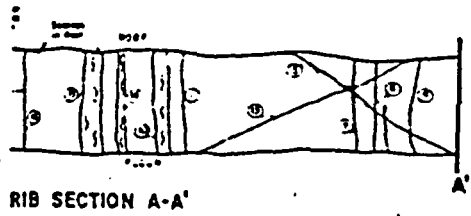
Each mapped discontinuity was labeled in the field and on the map in order to permit future checking or other use of the results. A short mark of about 30 cm was made along each mapped feature with fluorescent spray paint and a number was written in ink and circled to distinguish it from other labels on the rock. As previously mentioned, these marks are usually near eye level, except for certain discontinuous fractures that were only seen in the roof.

Clearly, sampling is biased in favor of fractures that are continuous and strike nearly perpendicular to the drifts. Fractures that are oriented parallel to the drifts are under-represented. Most of the low angle, fully healed joints were not mapped because they either did not intersect the floor, or were closed and thus less capable of conducting water. A more detailed geological or hydrological investigation would need to consider these biases.

RESULTS AND DISCUSSION

Results of the mapping are summarized by Fig. 5, which has been reduced from its original 1:60 scale. In order to provide maps suitable for future field work, enlargements of the composite portions indicated in Fig. 5 are given at a scale of 1:120 in Appendix A. A total of ninety features were sampled in the heater test alcove, access drift, and tail drift; and each is described in Appendix B according to its assigned number. Fig. 6 is an equal-area contour diagram of poles to the ninety fractures. Comparing this with the previous results reported for the Climax Stock in Fig. 3, there is general agreement in the predominant fracture or fault orientations. There appears to be some dissimilarity, however, in results for the tail and main access drifts, which is discussed further below.





- LEGEND**
- ① Non-shear fracture
 - ② Shear fracture
 - ③ Shear fracture (shear or fault)
 - ④ Shear fault
 - ⑤ Shear or fault zone
 - ⑥ Zone of fracture intersection
 - ⑦ Shear fracture (shear or fault)
 - ⑧ Fracture not reported in log
 - ⑨ Primary shear fracture
 - ⑩ Shear zone

MAIN ACCESS DRIFT

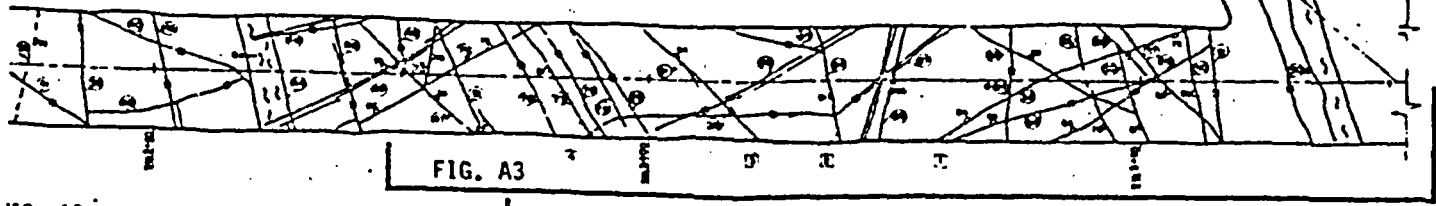


FIG. A2

FRACTURE MAPPING FOR RADIONUCLIDE MIGRATION PROGRAM	
[]	[]

Fig. 5. Floor map of major discontinuities in Tail and Main Access Drifts at 420m level of Climax Stock, NTS.

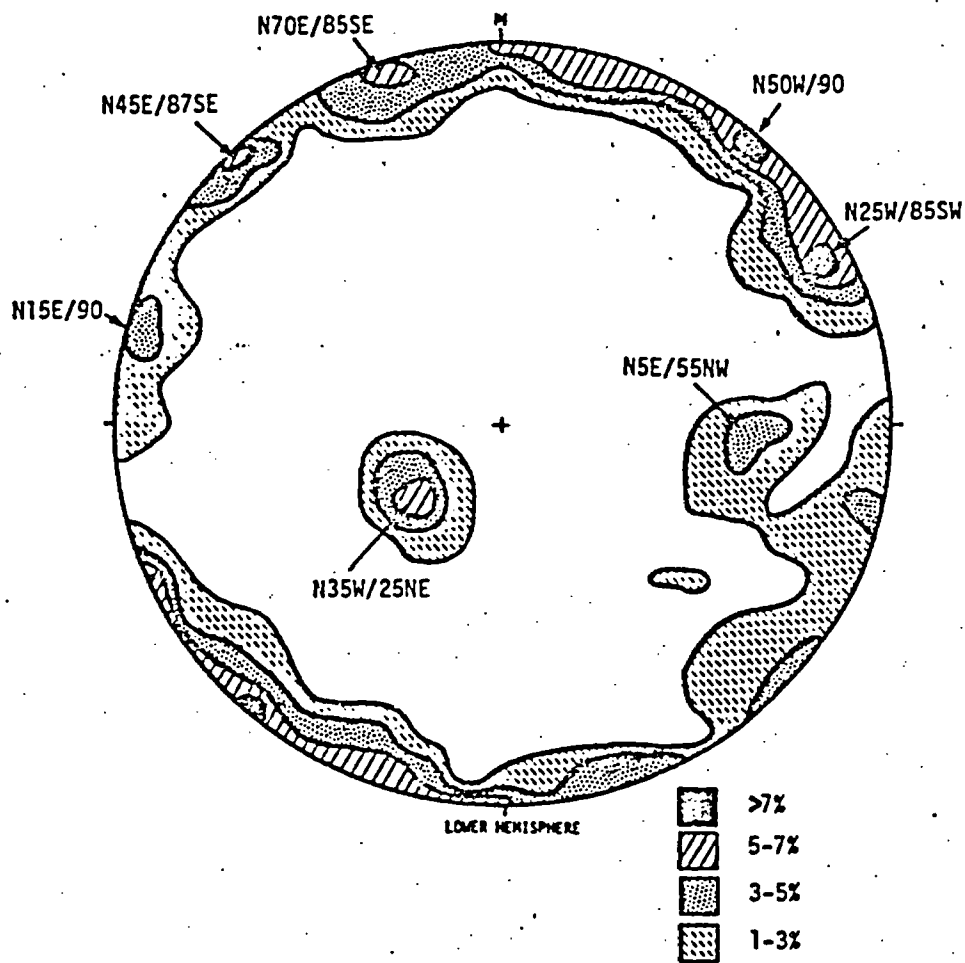


Fig. 6. Equal-area contour diagram of poles to 90 fractures mapped in the main access and tail drifts, based on data from Figs. 7 and 9. (Concentrations in percentage of points within on percent area counting circle).

Main Access Drift

Seventy-nine of the fractures mapped are located in the main access drift, and an equal-area pole plot of these is given in Fig. 7. In cases where a fracture is curved, the average of several different measured orientations was plotted. The predominant orientation of the fractures in the access drift is N50W/90 as indicated by Fig. 6. A somewhat lesser peak within this clustering is oriented N25W/85SW. These correspond roughly to the NW-striking fault and joint sets reported by Maldonado, as well as to some of the shear zones and joints given by Wilder and Patrick (1980). Typical mineralization of fractures in the main access drift is mostly calcite, with some iron oxide and chlorite. The wall rock is sometimes altered to clay. Thickness of filling varies widely both on a given fracture and among fractures, but for single, unsheared features it is typically one to three millimeters.

Seven fault zones within the N50W/90 set were mapped in the main access drift, all of which were identified in Maldonado's report. They are typically composed of many braided or en echelon fractures, and gouge material includes calcite, clay, and chlorite materials. Widths of the zones range from about 0.3 to 1.0 meter. A reliable direction of shearing could not be determined from the observed slickensides, though dip-slip motion is indicated. The wall rock is generally homogeneous, and because few other features were observed to cross these faults it was difficult to determine the amount of offset along the faults.

Another prominent grouping in Fig. 6 is oriented N45E/87SE and corresponds to the NE-striking set of high-angle fractures reported by Maldonado (1977) and Wilder and Patrick (1980). Two lesser modes occur near this set at N70E/85SE and N15E/90, however these do not correlate with previous mappings. Throughout most of the area mapped in the main access

Main Access Drift

Seventy-nine of the fractures mapped are located in the main access drift, and an equal-area pole plot of these is given in Fig. 7. In cases where a fracture is curved, the average of several different measured orientations was plotted. The predominant orientation of the fractures in the access drift is N50W/90 as indicated by Fig. 6. A somewhat lesser peak within this clustering is oriented N25W/85SW. These correspond roughly to the NW-striking fault and joint sets reported by Maldonado, as well as to some of the shear zones and joints given by Wilder and Patrick (1980). Typical mineralization of fractures in the main access drift is mostly calcite, with some iron oxide and chlorite. The wall rock is sometimes altered to clay. Thickness of filling varies widely both on a given fracture and among fractures, but for single, unsheared features it is typically one to three millimeters.

Seven fault zones within the N50W/90 set were mapped in the main access drift, all of which were identified in Maldonado's report. They are typically composed of many braided or en echelon fractures, and gouge material includes calcite, clay, and chlorite materials. Widths of the zones range from about 0.3 to 1.0 meter. A reliable direction of shearing could not be determined from the observed slickensides, though dip-slip motion is indicated. The wall rock is generally homogeneous, and because few other features were observed to cross these faults it was difficult to determine the amount of offset along the faults.

Another prominent grouping in Fig. 6 is oriented N45E/87SE and corresponds to the NE-striking set of high-angle fractures reported by Maldonado (1977) and Wilder and Patrick (1980). Two lesser modes occur near this set at N70E/85SE and N15E/90, however these do not correlate with previous mappings. Throughout most of the area mapped in the main access

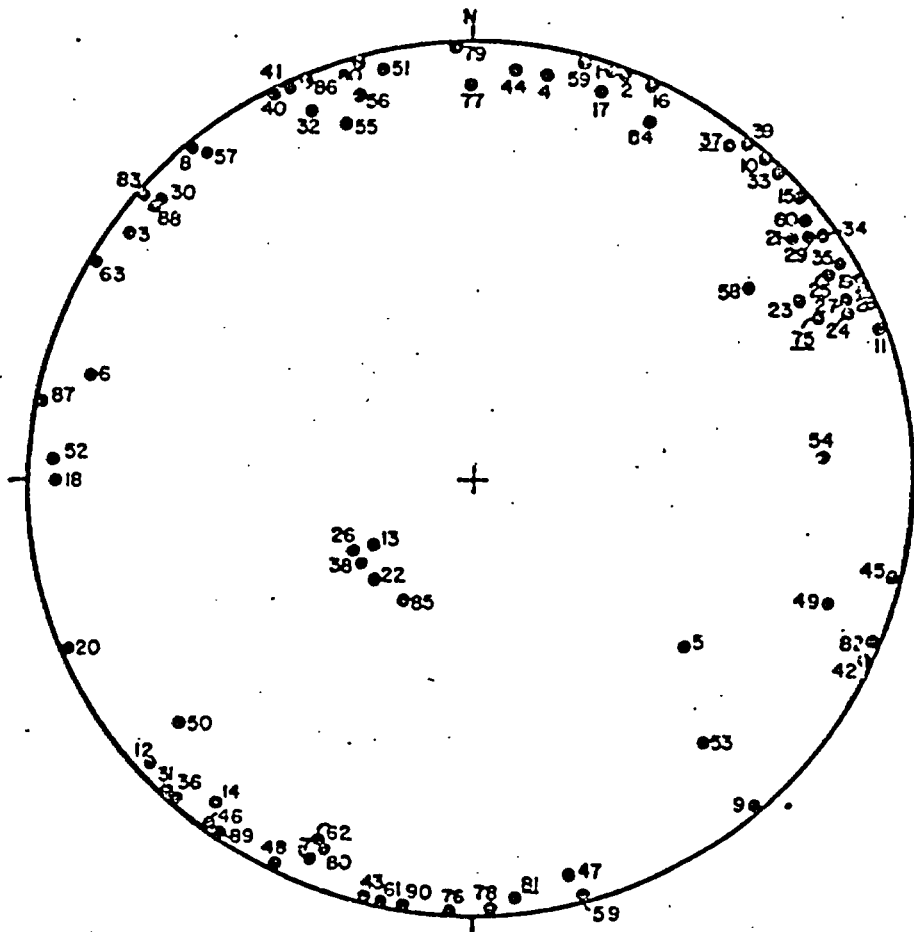


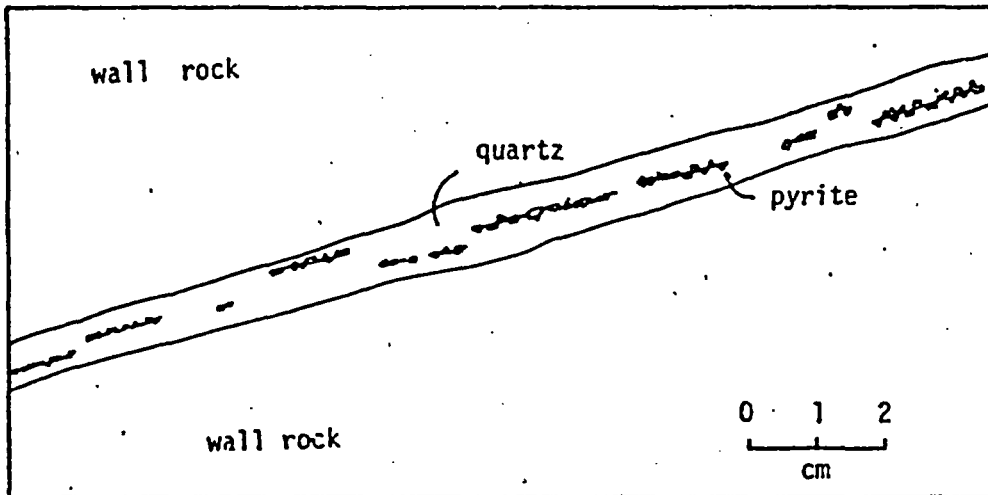
Fig. 7. Lower hemisphere Schmidt plot of poles to fractures mapped in the main access drift. Numbers correspond to features on base map; those underlined indicate average measurements on curved surfaces.

drift these fractures can be observed striking nearly parallel to the drift. Clearly, the sampling is geometrically biased against them, plus it is difficult to accurately measure orientations when the traces are in the roof of the tunnel. For the most part, fractures of this set were found to be quite variable in orientation (wavy) and discontinuous, which was not strictly in accordance with our sampling criteria. Therefore, a more detailed mapping effort in this area probably would yield a stronger clustering in Fig. 6.

A third set of discontinuities was observed in the access drift with a mean orientation of N35W/25NE. This sub-horizontal set is apparently pervasive in the Climax Stock, according to the data in Fig. 3. Most of these features are planar and healed by quartz up to 10 mm thick. They typically contain pyrite in either continuous veinlets or discontinuous stringers. As sketched in Fig. 8, they tend to break or be open where the pyrite is continuous. Some of these low-angle fractures in the vicinity of Sta. 1+50 (Section A-A' of Fig. 5) are apparently open and seeping groundwater. Collection of groundwater in this area is in progress as part of the geochemical characterization task (Isherwood, et al., 1980). An additional low-angle fracture with an orientation of N38E/52NW and several high-angle fractures are also seeping water; however, it is not clear which of these features is the dominant flow path.

In many places, the northeast-dipping, low-angle features are observed to truncate high angle fractures. Examples of this can be found in the rib map (Section AA') of Fig. 5. Evidence of faulting along the low-angle fractures is absent, and therefore would be an unlikely cause for the truncation. Our tentative explanation is that the low-angle discontinuities, either open or healed at the time, effectively blocked the propagation of the later high-angle fractures. Our data on such a relationship is indeed limited, and further detailed mapping would be needed to substantiate this explanation.

(a.)



(b.)

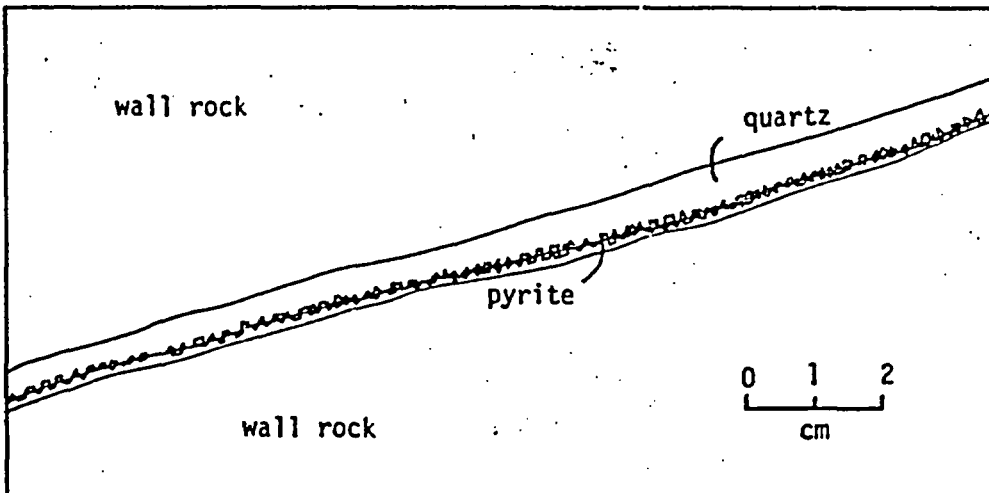


Fig. 8. (a) Low-angle healed fracture with discontinuous pyrite stringers. (b) Low-angle healed fracture with pyrite as a continuous layer. Open breaks or fissures tend to be along the continuous portions of the pyrite.

Tail Drift

Far fewer major fractures were found in the tail drift than in the main access drift. Only eleven were identified over a distance of about 30 meters (frequency = 0.37 fracture/m), whereas the main access drift yielded a frequency of 79/85 m = 0.93 fracture/m. Three of the major fractures fall into the NW-striking, high-angle set, and one belongs to the low-angle NE-dipping set of the Stock (Fig. 9). The remaining seven fractures have a mean orientation of about N5E/50NW, which lies outside the major NE-striking set described earlier. However, Wilder and Patrick (1980) report the latter as the dominant joint orientation in the tail drift, which would indicate that none of those joints apparently met the continuity or persistence criteria for our mapping. Orientation of the drift with respect to the NE-striking set would be of lesser importance in causing this bias.

The nature of the major NE-striking fractures in the tail drift appears to be somewhat different than that noted in the access drift. Their traces are typically more planar; and although the mineralization is similar (calcite, iron oxides, and chlorite), it is somewhat thicker at 5 to 20 mm.

RECOMMENDATIONS

In terms of potential fracture sites for radionuclide migration tests, several areas appear promising. First, in the main access drift there are several features near the heater test drift that could probably be intercepted at some suitable distance from the drift by horizontal boreholes. As members of the main set (N50W/90) in the drift, at least four fractures could be intersected by a pair of 8 m boreholes. On the base map these are numbered 1

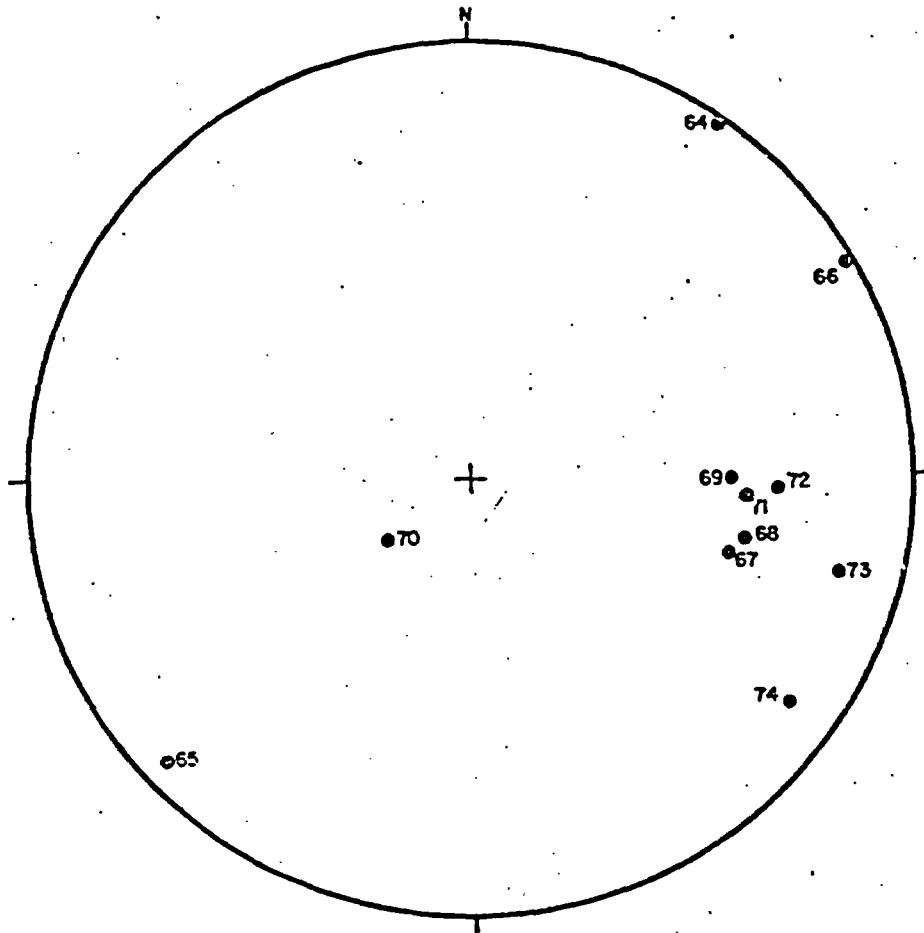


Fig. 9. Lower hemisphere Schmidt plot of poles to fractures mapped in the tail drift.

through 4. (They should not be confused with fractures currently being studied in the Radionuclide Migration Program.) Also in this area, a major low-angle, water bearing fracture (number 5) could be intercepted with a slant-drilled borehole. This would provide an opportunity to develop testing capabilities for non-vertical fractures, if the need arises in the future.

A second pair of candidate fractures is in the tail drift, oriented N50E/vertical. These fractures may be more conductive than desirable for the migration experiments; however, the relatively few number of major intersecting fractures in the drift makes this area attractive for single-fracture flow studies.

We would recommend that the major fault zones in the access drift near stations 1+35, 1+80, 2+30, 2+60, and 3+65 be avoided for the type of single-fracture work under the current work plan. However, faults are very important hydrologic features and these would be excellent sites for studying flow through them. In terms of an underground repository of nuclear waste, highly fractured zones will require special attention when encountered, and development of techniques for characterizing their transport properties could be accomplished in the Climax Stock.

ACKNOWLEDGMENTS

The authors wish to thank Dana Isherwood for support in this work, as well as Dale Wilder and Jesse Yow, Jr., for their constructive reviews of the report. We are also grateful to Priscilla Proctor for her help in drafting the figures, and to Lydia Burrow for typing the manuscript.

REFERENCES

Barnes, H., Houser, F. N., and Poole, F. G., 1963 Geologic Map of the Oak Spring Quadrangle, Nye County, Nevada, USGS Geol. Quad. Map GQ-214.

Carlson, R., W. Patrick, D. Wilder, W. Brough, U. Montan, P. Harben, L. Ballou, and H. Heard, 1980, Spent Fuel Test - Climax: Technical Measurements interim report, FY 1980. Lawrence Livermore National Laboratory, UCRL-53064, 104 pp.

Compton, Robert R., 1962, Manual of Field Geology, John Wiley & Sons, NY.

Houser, F. N., and F. G. Poole, 1960, Preliminary Geologic Map of the Climax Stock and Vicinity, Nevada Test Site, Nye County, Nevada.

Houser, F. N., and F. G. Poole, 1961, Age Relations of the Climax Composite Stock, Nevada Test Site, Nye County, Nevada, USGS Professional Paper 424B, p B176-177.

Isherwood, D., E. Raber, D. Coles, and R. Stone, 1980, Program Plan: Field Radionuclide Migration Studies in the Climax Granite. Lawrence Livermore National Laboratory, UCID-18838, 60 pp.

Ramspott, et al., 1979, Technical Concept for a Test of Geologic Storage of Spent Reactor Fuel in the Climax Granite, Nevada Test Site, Lawrence Livermore National Laboratory, UCRL-52796.

Maldonado, F., 1977, Summary of The Geology and Physical Properties of the Climax Stock, Nevada Test Site, USGS Open File Report 77-356.

Wilder, D. G. and W. C. Patrick, 1980, Geotechnical Status Report for Test Storage of Spent Reactor Fuel in Climax, Granite, Nevada Test Site. Lawrence Livermore National Laboratory, UCRL-85096.

APPENDIX A - ENLARGED FRACTURE MAPS FROM FIG. 4

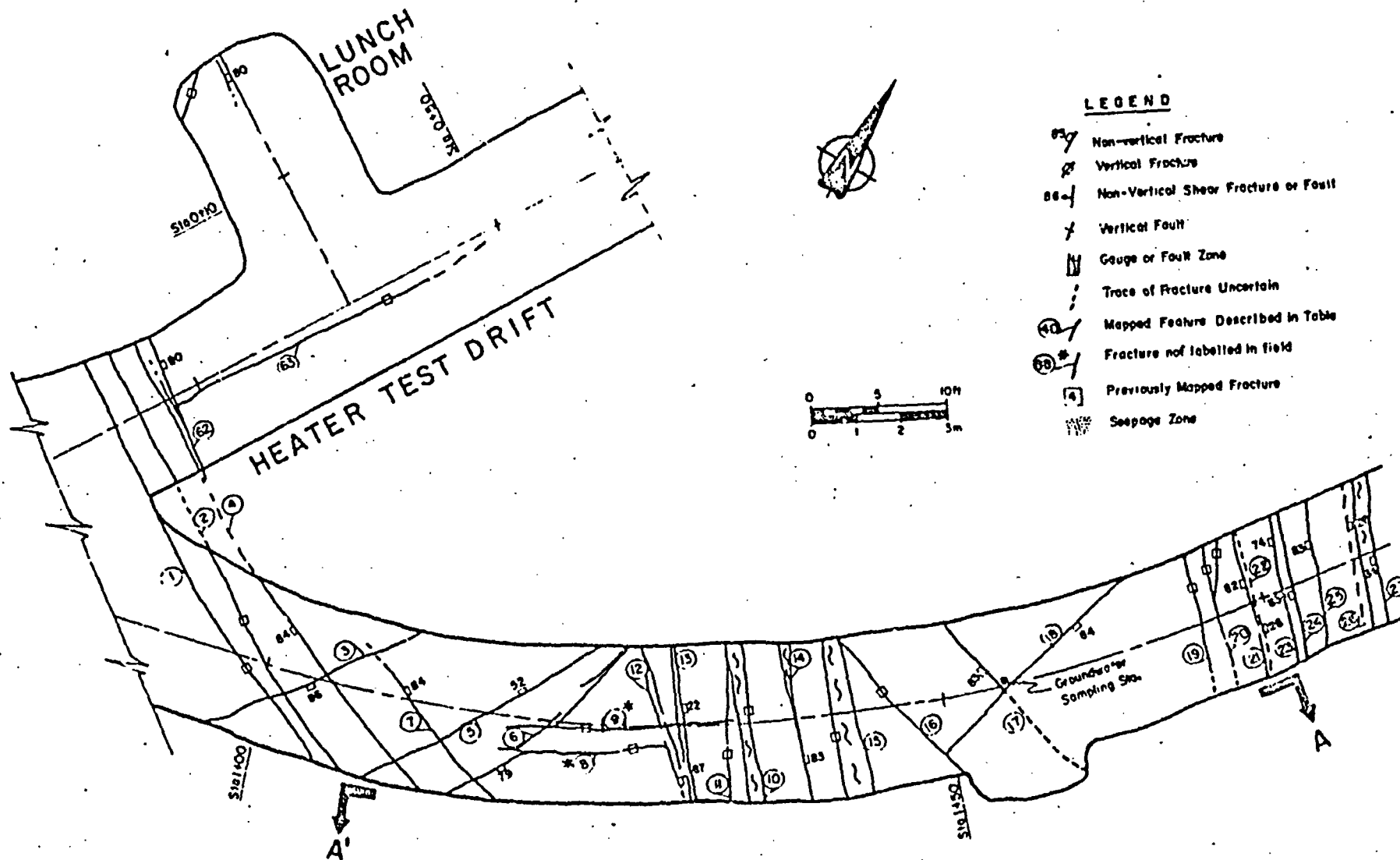


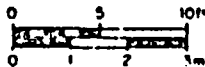
Fig. A1. Floor map of Heater Test Drift and Main Access Drift from station 0+90 to 1+85.

Fig. A2. Floor map of Main Access Drift
from station 1+80 to 2+85.



LEGEND

- Non-vertical Fracture
- Vertical Fracture
- Non-Vertical Shear Fracture or Fault
- Vertical Fault
- Gauge or Fault Zone
- Trace of Fracture Uncertain
- Mapped Feature Described in Table
- Fracture not labelled in field
- Previously Mapped Fracture
- Seepage Zone



PILEDRIVER MAIN ACCESS DRIFT

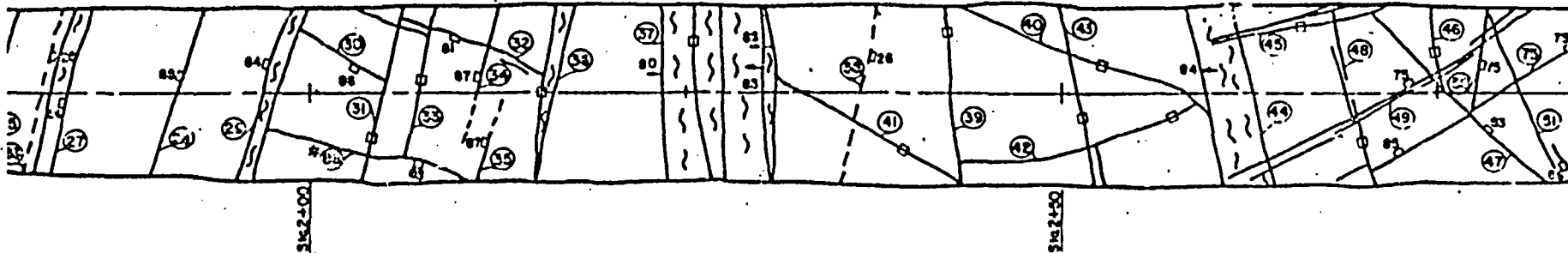
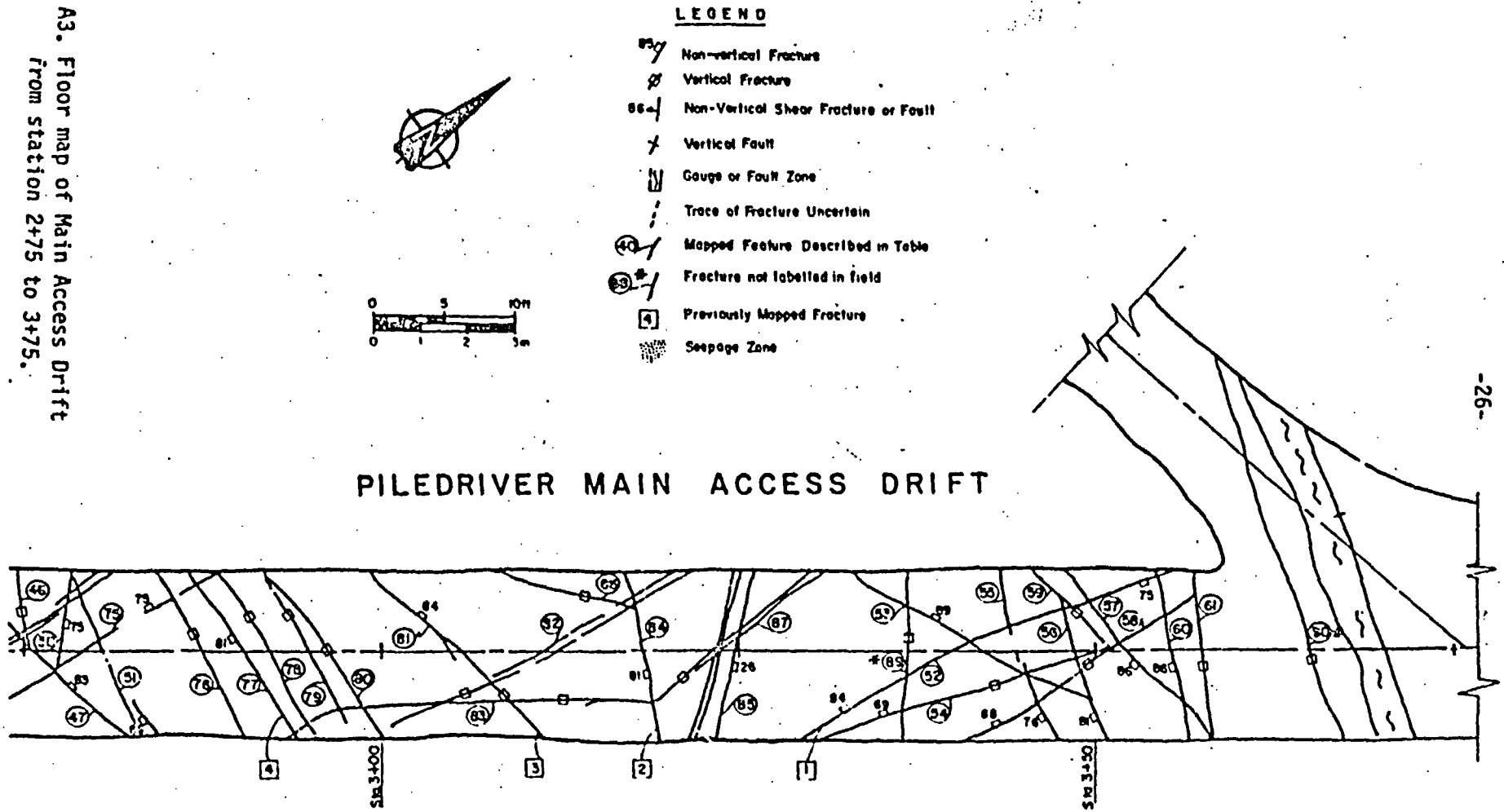
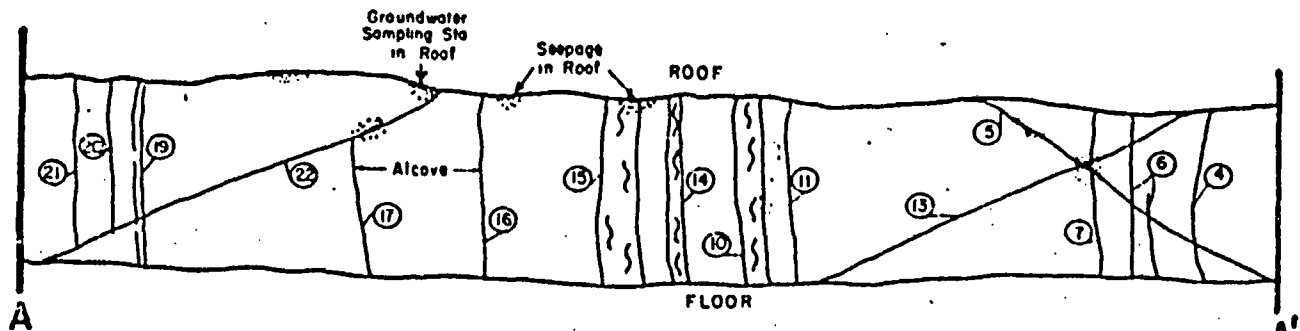


Fig. A3. Floor map of Main Access Drift
from station 2+75 to 3+75.

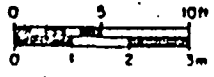




RIB SECTION A-A'

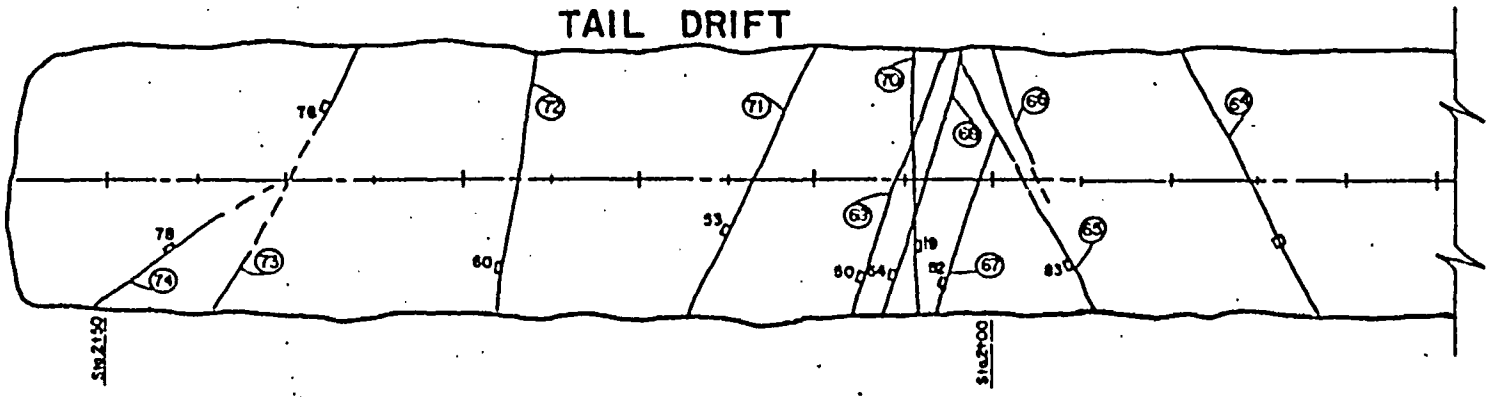
LEGEND

- Non-vertical Fracture
- Vertical Fracture
- Non-Vertical Shear Fracture or Fault
- Vertical Fault
- Gauge or Fault Zone
- Trace of Fracture Uncertain
- Mapped Feature Described in Table
- Fracture not labelled in field
- Previously Mapped Fracture
- Seepage Zone



-27-

Fig. A4. Tail Drift floor map and south rib map in vicinity of station 1+50.



APPENDIX B - TABLE OF DESCRIPTIVE FRACTURE DATA

NO. ON MAP	APPROX. STATION	ORIENTATION		TYPE OF DISCONTINUITY			MINERALIZATION		REMARKS	
		STRIKE (DEGREES)	DIP (DEGREES)	SINGLE FRACTURE	ZONE WIDTH (cm)	CONTINUOUS	DISCONT./TRUNCATED	TYPE(S) C= Calcite F= Fe Ox. P= Pyrite K= Chlorite A= Clay		FILLING THICKNESS (mm)
1	0+97	N72W	~90		2-15	X		C,F	2-3	
2	0+99	N70W	~90		2-15	X		C,F	2-3	
3	1+04	N36E	86SE		X	X		C,F	1-2	
4	1+06	N80W	84SW		X		X	C,F	2-5	
5	1+14	N38E	52NW	X		X		C	2-3	Seepage SE rib
6	1+22	N16E	79SE		20-30		X	C	1-3	
7	1+10	N67W	84NE	X			X	C	2-3	
8	1+25	N50E	~90		X		X	C,F	1-2	Strike uncertain
9	1+25	N51E	~90		X		X	C,F	1-2	Strike uncertain
10	1+35	N19W	~90		30	X		C	1-2	Shear zone
11	1+34	N22W	~90	X			X	C	1-2	Splay off 10
12	1+30	N42W	87NE		X		X	C	1-2	Obscure trace
13	1+31	N34W	22NE	X		X		C	1-5	Partly healed; Qtz
14	1+34	N52W	83NE		5-10	X		C,F	1-3	
15	1+43	N42W	~90		10	X		C,F	2-10	Unaltered Biotite
16	1+46	N66W	~90	X		X		C	1-3	
17	1+54	N77W	83SW	X			X	C,F	1	Healed
18	1+55	N-S	84E	X			X	C,F	1-3	
19	1+70	N29W	~90		1-5	X		C	1-3	
20	1+71	N23W	~90	X			X	C	1-5	Splay in NW rib
21	1+74	N37W	82SW	X			X	C,F	1-3	
22	1+74	N46W	26NE	X		X		C,F	1-5	Truncates others
23	1+76	N29W	74SW		X	X		C,A	50-100	Gouge zone
24	1+77	N24W	83SW		X	X		C,A	50-100	Gouge zone
25	1+79	N30W	83SW		X	X		C,F,A	20-50	Gouge zone
26	1+82	N31W	26NE	X			X	C,F	1-5	Qtz
27	1+83	N26W	84SW		X	X		C,F,A	10-50	Gouge zone
28	1+91	N27W	88SW	X				C,F	2-10	
29	1+97	N36W	84SW		10-50			C,F,A	5-30	Some gouge
30	2+02	N42E	85SE	X			X	F	1-2	Strike uncertain
31	2+04	N46W	~90		2-3	X		C,F	2-3	
32	2+10	N67E	81SE		2-5		X	C,F	1-5	Strike uncertain
33	2+07	N47W	~90		X		X	C,F	1-2	
34	2+11	N35W	87SW		10-15		X	C,F,A	10-20	Gouge zone
35	2+12	N31W	87SW		1-2		X	C	1-2	

NO. ON MAP	APPROX. STATION	ORIENTATION		TYPE OF DISCONTINUITY			MINERALIZATION		REMARKS	
		STRIKE (DEGREES)	DIP (DEGREES)	SINGLE FRACTURE	ZONE WIDTH (cm)	CONTINUOUS	DISCONT./ TRUNCATED	TYPE(S) C= Calcite F= Fe Ox. P= Pyrite K= Chlorite A= Clay		FILLING THICKNESS (mm)
36	2+16	N46W	~90		5-30	X		C,F,A	10-30	Some gouge
37	2+23	N42W	80SW			X		C,K,A		Fault zone
"	2+25	N51W	~90							2+23 to 2+31
"	2+30	N55W	85SW							
"	2+31	N59W	86SW							
38	2+37	N37W	26NE	X			X	C,F	2-3	Partly healed; Qtz
39	2+42	N57W	~90		X	X		C,A	1-20	Gouge
40	2+50	N63E	~90	X			X	C,F	10-20	
41	2+36	N65E	~90		5-10		X	C	2-3	
42	2+51	N25E	~90		5-20		X	C,F	1-5	Irreg. zone
43	2+51	N75W	~90		10-50		X	C,F		
44	2+61	N84W	84SW		100	X		C,F	1-10	Fault zone
45	2+65	N12E	~90		X		X	C,F	1-2	
46	2+74	N52W	~90	X			X	C,F	1-10	Splay off 47
47	2+75	N76E	83NW		1-5	X		C,F,A	<20	Gouge zone
48	2+69	N62W	~90		X		X	C,F	2-3	
49	2+72	N19E	75NW		5-10		X	C	2-3	
50	2+77	N40W	75NE	X			X	C,F	1-5	Splay off 47
51	2+80	N78E	85SE		X		X	C,F	1-2	
52	3+40	N05E	84NW		5-30	X		C,F	2-3	FR. #1 of previous mapping
"		N02E	75SE							
53	3+41	N48E	69NW	X			X	C		
54	3+45	N04W	69SW		10		X	C	1-2	Orient. varies
55	3+44	N71E	76SE		X	X		C	1-3	Strike uncert.
56	3+48	N74E	81SE		X		X	C	1-2	Strike uncert.
57	3+51	N51E	86SE	X		X		C	1-3	
58	3+50	N35W	66SW	X			X	C,F	1-3	Orient. varies
59	3+50	N75E	~90	X			X	C	1-3	
60	3+55	N38W	86SW	X		X		C,F		Orient. uncert.
61	3+57	N78W	~90	X		X		C,F,A	5-10	Gouge
62	0+23(HD)	N68W	80NE	X		X		C	1-5	
63	0+30(HD)	N30E	~90		X		X	C	1-3	
64	1+85(TD)	N55W	~90		1-2	X			1-5	Some quartz
65	1+98(TD)	N43W	83SW		3-5	X		K,F	2-5	
66	1+97(TD)	N30W	~90	X			X			

END-

DATE FILMED

09/02/81